Journal of Applied Polymer Science

PLA/functionalized-gum arabic based bionanocomposite films for high gas barrier applications

Neelima Tripathi, Vimal Katiyar
Department of Chemical Engineering, Indian Institute of Technology Guwahati, Guwahati, Assam, India
Correspondence to: V. Katiyar (E-mail: vkatiyar@iitg.ernet.in)

ABSTRACT: The present work focuses on the microwave synthesis of lactic acid-*grafted*-gum arabic (LA-*g*-GA) by polycondensation reaction and its influence as an additive to improve the gas barrier properties of poly(lactic acid) (PLA) films, prepared by solution casting method. It is observed that during the synthesis of LA-*g*-GA, hydrophilic gum is converted into hydrophobic due to grafting of *in situ* grown hydrophobic *oligo*-(lactic acid). Subsequently, PLA/LA-*g*-GA bionanocomposite films are fabricated and characterized for structural, thermal, mechanical and gas barrier properties. Path breaking reduction in oxygen permeability (OP) of ~10 folds is achieved in case of PLA films containing LA-*g*-GA as filler. However, water vapor transmission rate (WVTR) is reduced up to 27% after 5 wt % addition of filler. Reduction in OP of this order of magnitude enables the PLA to compete with PET in term of enhancing shelf life and maintaining the food quality. © 2016 Wiley Periodicals, Inc. J. Appl. Polym. Sci. **2016**, *133*, 43458.

KEYWORDS: biopolymers and renewable polymers; composites; films; grafting; packaging

Received 30 September 2015; accepted 18 January 2016
DOI: 10.1002/app.43458

INTRODUCTION

The demand of polymeric materials is exponentially growing compared to conventional materials due to their remarkable properties such as low density, chemical resistance, low toxicity, and low cost. The global polymer production in 2050 is approximated around 300 million tons.[1] The use of plastics in packaging applications is increasing day by day. Among the different types of packaging materials, food-packaging materials play a vital role in extending shelf-life and for maintaining the quality of food. Most of the food packaging materials are made from the petroleum-based polymers due to their large-scale availability, good gas barrier, and mechanical properties. In spite of several advantages, these petroleum-based polymeric materials have certain limitations such as poor biodegradability and non-renewability.[1,2] To overcome such limitations, development of bio-based, renewable, and biodegradable packaging materials have been emerging day by day.

Bio-based polymers based on their origin of raw materials and synthesis process can be classified into three categories namely (i) extracted from biomass, (ii) synthesized from bio-derived monomers, and (iii) produced from microorganisms.[3,4] These polymeric materials can be degraded after their service life. However, these materials also have certain limitations, such as inferior thermal properties, poor gas barrier, and low mechanical properties.[2] Different bio-based polymers used in packaging applications are poly(ε-caprolactone) (PCL), poly(hydroxyl alkanoates) (PHAs), and poly(ethylene glycol) (PEG), whereas poly(lactic acid) (PLA) is a promising bio-based, renewable, and biodegradable thermoplastic polyester derived from lactic acid (2-hydroxy propionic acid) which can be used for the preparation of eco-friendly packaging materials.[5,6] PLA is the first renewable bio-based synthetic polymer that has been exploited for commercialization at large scale.[7,8] Across the wide range of applications, it offers a sustainable alternative to polymeric materials used for food packaging, because of its advantages as high transparency, processability, and rigidity with relatively low crystallization rate.[9] On the other hand, some of the characteristic properties of PLA, that are considered inadequate for its application as a food packaging material, are poor heat stability, inferior mechanical properties and low gas barrier properties with respect to current petroleum-based polymers such as polyethylene terephthalate.[5] However, PLA could be employed to make better packaging materials by modifying it with other natural polymeric materials, such as cellulose, chitosan, clay and many more.[10–13]

Polysaccharide gums are natural biopolymer, which are abundantly available in nature. These gums find tremendous industrial applications in various fields due to their renewability, non-toxicity, and biodegradability. Gum Arabic (GA) is a complex polysaccharide which is obtained as an exudate from Acacia trees such as *Acacia senegal* and *Acacia seyal*.[14] The polydisperse GA molecule has three main fractions namely, arabinogalactan (AG), arabinogalactan-protein (AGP), and glyco-protein (GP). The

gum is composed of approximately 90% AG fraction (which has very little associated protein), around 10% AGP fraction (which contains ~10% of protein component), and about 1% GP fraction (which contains ~20–50% of protein component).[15,16] GA is a non-toxic hydrophilic biopolymer in its natural form which has good emulsion and encapsulation properties.[17] It can also be used as a filler with some modifications in its structural properties for decreasing the gas-transport through the films. The gas-transport process is defined by permeability, diffusion, and solubility coefficients. At steady state, permeability can be expressed by the product of diffusion and solubility coefficients. The initial increment in permeability values with time is only governed by diffusion process, which decreases with increase in tortuosity and the increase in tortuosity is due to the incorporation of filler in polymer matrix. Hence, increase in tortuosity has the great impact on increasing the shelf-life of the products in food packaging applications.[18] Oxygen permeability (OP) depends on many interrelated factors such as hydrogen bonding characteristics, degree of branching or cross-linking between polymeric chains, molecular weight, polarity, and structural features of polymeric side chains, processing methodology, degree of crystallinity, and method of synthesis.

Literature survey reveals that none of the articles has demonstrated the blends of PLA and lactic acid-*grafted*-gum arabic (LA-*g*-GA) for film preparation for packaging application. It might be due to incompatibility of pristine PLA, which is hydrophobic whereas GA is hydrophilic in nature. Hence in the present study, PLA is blended with varying proportions of hydrophobic LA-*g*-GA (also referred as filler) were used for the preparation of 'green' films by solution casting approach. Various analyses such as structural, thermal, mechanical, surface morphology, and barrier properties of films were studied in detail. One of the major objectives of the present investigation is to develop a novel and ecofriendly packaging material with improved gas barrier properties.

EXPERIMENTAL

Materials

L-lactic acid and poly(lactic acid) (PLA) (granular form; 2003D; density: 1.24 g cm^{-3}) were procured from Purac, India and NatureWorks, respectively. Gum Arabic (GA) from acacia tree (branched polysaccharide) and deuterated chloroform ($CDCl_3$) were procured by Sigma-Aldrich (India). Chloroform (extra pure, Merck, India) was used as a solvent for film fabrication and chloroform (high performance liquid chromatography (HPLC) grade, Merck, India) was used for analysis.

Methods

Preparation of Lactic Acid-*grafted*-Gum Arabic (LA-*g*-GA) Filler. The synthesis of LA-*g*-GA was done by polycondensation reaction. In this process, LA and GA were taken in the proportion of 5:1 (wt/wt) and manually mixed in the round bottom flask (RBF) before synthesis. The RBF was fixed in microwave reactor and nitrogen gas was passed into the RBF to maintain the inert atmosphere. Microwave condition was adjusted to 'convection cum microwave' mode with set temperature at 130 °C and the reaction was conducted for 45 minutes at 240 watts. The temperature of the heating belt, connected between RBF outlet and condenser, was maintained at 100 °C to avoid condensation of byproducts. Finally, the synthesized material i.e. LA-*g*-GA was converted into solid form upon cooling which was kept for further analysis, as shown in scheme 1. The *oligo*-(L-lactic acid) (OLLA) was prepared at same operating conditions in microwave reactor.

Preparation of PLA/LA-*g*-GA Bionanocomposite Films. PLA/LA-*g*-GA bionanocomposite films with 3, 5, and 10 wt % loading of LA-*g*-GA filler were prepared by solution casting method. Solutions of PLA/LA-*g*-GA films were prepared by dissolving LA-*g*-GA with PLA granules in chloroform with vigorous stirring magnetically at room temperature. The solutions were poured into 15 cm diameter Teflon petri dishes to obtain the films after evaporation of solvent. PLA films were also prepared by the same procedure. The formed films were peeled off from the Petri dishes after 12 hours and further dried in vacuum oven at 40 °C for 12 hours to remove the remaining chloroform from the films. The thickness of the different films (PLA, PLA/LA-*g*-GA (3%), PLA/LA-*g*-GA (5%), and PLA/LA-*g*-GA (10%) were determined by thickness meter at ten different locations

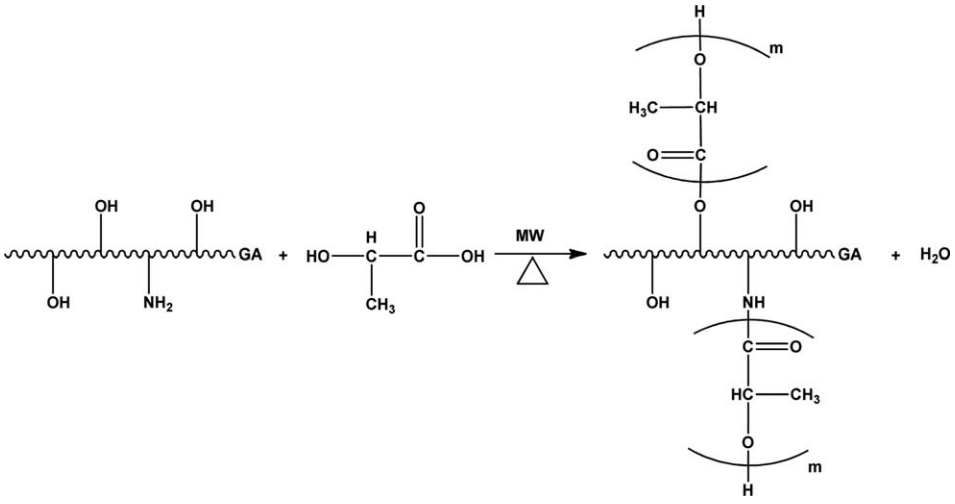

Scheme 1. Schematic representation of the synthesis of LA-*g*-GA.

Table I. Composition of Blends and Thickness of Their Films

Codes of film samples	Composition of blends		Film thickness (μm)
	PLA (wt %)	LA-g-GA (wt %)	
PLA	100	0	100.0 ± 2
PLA/LA-g-GA (3%)	97	3	102.5 ± 3
PLA/LA-g-GA (5%)	95	5	85.8 ± 5
PLA/LA-g-GA (10%)	90	10	89.5 ± 8

and the average values were calculated and summarized in Table I.

Material Characterization

^{1}H-NMR Analysis of LA-*g*-GA. Nuclear magnetic resonance (NMR) analysis was performed for OLLA and LA-*g*-GA samples by using Bruker Ascend™ 600 nuclear magnetic resonance spectrometer. The samples were prepared by dissolving 5–10 mg/mL in deuterated chloroform ($CDCl_3$). The solution was filtered by using 0.45 μm size syringe filter before analysis. Further, the solutions were transferred into NMR tubes for analysis, which was done in the spectral range of 0 to10 ppm at room temperature.

Attenuated Total Reflectance-Fourier Transform Infrared Spectroscopy Analysis (ATR-FTIR). Attenuated total reflectance-Fourier transform infrared spectroscopy (ATR-FTIR) was carried out by using IRAffinity-I Shimadzu spectrophotometer. The spectra from PLA, PLA/LA-*g*-GA (3%), PLA/LA-*g*-GA (5%), and PLA/LA-*g*-GA (10%) bionanocomposite films were recorded in transmission mode within a wavenumber range of 4000–600 cm^{-1} at averaging a minimum of 20 scans with a resolution of 4.0 cm^{-1}. Film samples were kept at 80 °C for 2 hours in hot air oven before analyzing.

X-ray Diffraction (XRD) Analysis. X-ray diffraction (XRD) analysis was carried out by using X-ray diffractometer (Bruker, D8 Advance). The CuKα radiation source ($\lambda = 1.54$ Å, power/applied voltage = 40 kV) was used. XRD patterns were observed between 2° and 50° with scan speed of 2 sec/step and increment of 0.05°/sec. The films were kept in hot air oven at 80 °C for 2 hours before analysis. Segal empirical method was used to calculate the crystallinity index (Cr I) by employing the following expression:

$$\text{Cr I} = \frac{(I_{[110/200]} - I_{am})}{I_{[110]/[200]}} \times 100 \quad (1)$$

where I is the maximum intensity of the lattice reflection of PLA crystallography at around $2\theta = 16.7°$ and I_{am} is the intensity of diffraction of the amorphous material at minimal intensity.[19–21]

Thermogravimetric Analysis (TGA). The thermal stability of the all film samples was determined by thermogravimetric analysis (TGA) with a PerkinElmer Simultaneous Thermal Analyzer (STA-8000). The analysis was conducted in the temperature range from 35 °C to 500 °C at 5 °C/min heating range under inert atmosphere.

Differential Scanning Calorimetry (DSC). Differential scanning calorimetry (DSC) was carried out in DSC 1, Star^e System, METTLER TOLEDO. The analysis was performed in inert atmosphere. Aluminum crucibles were used for the tests, where reference crucible was placed empty. Samples were heated from −25 °C to 200 °C at 5 °C/min heating rate. After erasing the processing history in first heating cycle, samples were again cooled to −25 °C and then second heating cycles were recorded.

Surface Morphology. Transmission electron microscope (TEM, JEOL, JEM-2100) was used for analyzing the film samples. For preparing the sample, small piece of thin film was dissolved in the HPLC grade chloroform. Then the solution was filtered using Whatman® syringe filter (pore size 0.45 μm). Thereafter, a drop of the filtered solution was put on the copper grid. The solvent was allowed to evaporate for 12 hours at room temperature before analysis.

Mechanical Properties. A universal testing machine (UTM) (Kalpak Instruments and Controls, model KIC-2-050-C) was used to determine different mechanical properties such as tensile strength (MPa), Young's modulus (MPa), and elongation at break (%). Film samples were cut as strips with 100 mm length and 25.4 mm width according to ASTM D882-02. The samples were equilibrated in an environmental chamber for 48 hours at 50 ± 5% relative humidity (RH) and 25 ± 5 °C temperature before testing. A 1000 N load cell was used for tensile test. Cross-head speed was 50 mm/min and the grip separation was set at 50 mm.

Oxygen Permeability. Oxygen transmission rate (OTR) measurements were carried out by using an oxygen permeability tester (Labthink, model PERME® OX2/231) according to ASTM standard D3985. The temperature was maintained by using the temperature controller (Labthink, model TC-01). The test was conducted at 25 ± 0.1 °C and 0% relative humidity (RH). The test area considered for analyzing the samples was 50 cm^2. While analyzing the sample, pure nitrogen (99.9995%) was passed in the lower half of the chamber and pure oxygen (99.95%) was introduced in the upper half of the chamber. Film thickness was measured with digital coating thickness meter (model indi6156; indi). The thickness of each sample was determined at 10 different locations and their average value was considered. The OTR (cm^3 m^{-2} day^{-1}) values were recorded. The tests were performed in duplicate and the average values have been reported. The OTR value obtained from the instrument was multiplied by the average film thickness (e, in mm) for each film, and expressed as OTR × e values (cm^3 mm m^{-2} day^{-1}).

Water Vapor Transmission Rate (WVTR). Water vapor transmission rate (WVTR) of the films was calculated according to the ASTM E398 by water vapor permeability tester (Mocon, PERMATRAN-W® 1/50G). Prior to the analysis, the sample was conditioned at 25 ± 1 °C and 50% RH for 48 hours. The test was conducted for exposure area of 50 cm^2 at 37.8 ± 0.5 °C and 100% RH. Nitrogen gas (99.9% purity) was purged through the films during the analysis. The test was performed at continuous mode. The test readings were noted down after reaching the saturation point of WVTR value. The tests were performed in

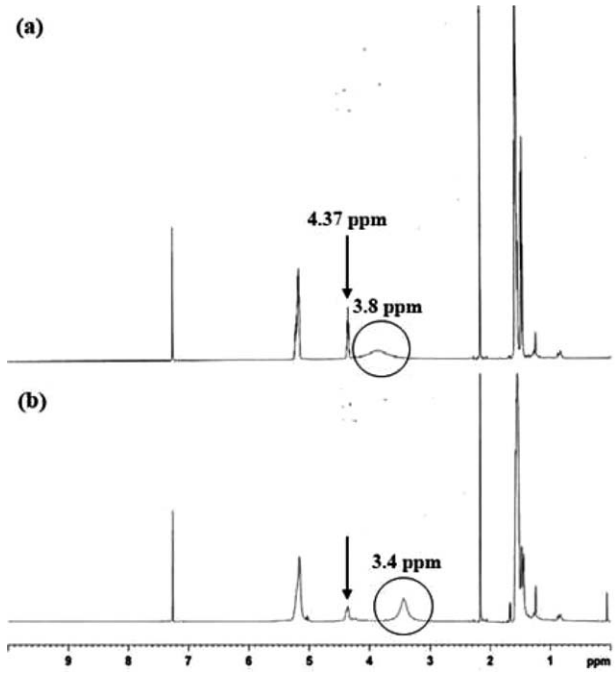

Figure 1. ^{1}H-NMR analysis of (a) OLLA and (b) LA-*g*-GA.

triplicate and the average values have been reported. The WVTR value obtained from the instrument was multiplied by the average film thickness (e, in mm) for each film, and expressed as WVTR × e values (cm^3 mm m^{-2} day^{-1}).

RESULTS AND DISCUSSION

^{1}H-NMR Analysis of LA-*g*-GA

The ^{1}H-NMR spectra of OLLA and LA-*g*-GA are shown in Figure 1. The common peaks are observed at 1.4, 4.3, and 5.2 ppm, which assign the methyl protons of the OLLA side chain, terminal -C(CH_3)H- group, and -CH- hydrogen of lactyl moiety respectively. Moreover, the intensity of signals at 4.37 ppm reduces with increase in filler concentration, which suggests the grafting of OLLA on -NH_2 group of GA. Further, the grafting phenomena was also confirmed by the intensity variation and shifting of the peak from 3.8 to 3.4 ppm.[22]

Chemical Interaction Analysis

ATR-FTIR spectra of neat PLA and PLA/LA-*g*-GA films with varying loadings of LA-*g*-GA were recorded, as shown in Figure 2. In the spectrum of neat PLA films, the peak at 869 cm^{-1} assigned to -C-C- stretch; and peaks at 1083 cm^{-1}, 1130 cm^{-1}, and 1182 cm^{-1} assigned to -C-O- bond stretching of -CH-O- group. The peaks at 1359 cm^{-1}, 1382 cm^{-1}, and 1454 cm^{-1} were attributed to -CH_3 angular deformation, -CH- deformation (including symmetric and asymmetric bend), and -CH_3 bend, respectively. The band originated from -C=O stretching vibration of carbonyl is situated at 1747 cm^{-1}. In the spectra of PLA/LA-*g*-GA films, a new peak originated at 1755 cm^{-1} also corresponds to -C=O stretching vibration due to oligomer molecules.[23] It was observed that with increase in the concentration of LA-*g*-GA, peak intensity at 1747 cm^{-1} decreased.

Crystal Structure Analysis

Figure 3 showed the diffraction patterns of all the four film samples (PLA, PLA/LA-*g*-GA (3%), PLA/LA-*g*-GA (5%), and PLA/LA-*g*-GA (10%)). For neat PLA film, crystalline peaks were observed at $2\theta = 14.9$, 16.7, 19.1, and 22.3 which attributed to [0 1 0], [1 1 0]/[2 0 0], [2 0 3], and [0 1 5] reflections, respectively. The maximum intensity of peak at ~16° corresponds to the α-form of crystals, which confirmed that an ordered structure was still retained in all the film samples. The decrease in peak intensity was observed for PLA/LA-*g*-GA (3%) ($I_{max\ at\ 16.75°} = 403$) and PLA/LA-*g*-GA (5%) ($I_{max\ at\ 16.75°} = 737$) films with respect to neat PLA film ($I_{max\ at\ 16.7°} = 996$). Further, the values of Cr I for PLA, PLA/LA-*g*-GA (3%), PLA/LA-*g*-GA (5%), and PLA/LA-*g*-GA (10%) films as calculated by using eq. (1) were 87.95, 81.89, 86.43, and 88.34%, respectively. On comparing the XRD patterns of PLA/LA-*g*-GA (3%), PLA/LA-*g*-GA (5%), and PLA/LA-*g*-GA (10%) films, increase in peak intensity was observed with increase in filler loading. This increase in peak intensity could be attributed to the increase in crystallinity caused due to nucleating effect of LA-*g*-GA filler in the film

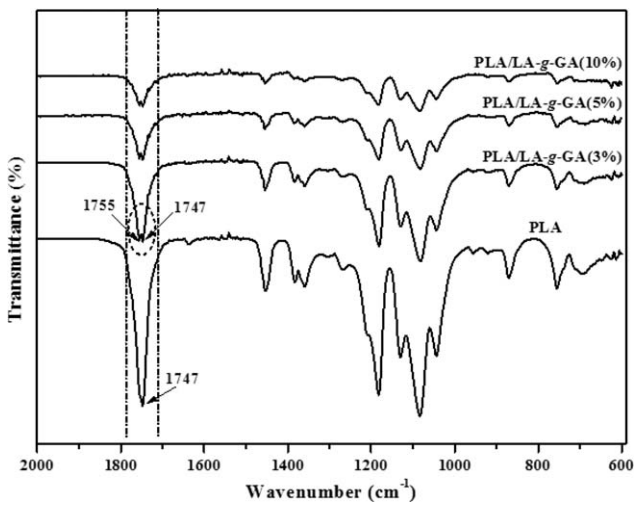

Figure 2. FTIR spectra of PLA, PLA/LA-*g*-GA (3%), PLA/LA-*g*-GA (5%), and PLA/LA-*g*-GA (10%) bionanocomposite films.

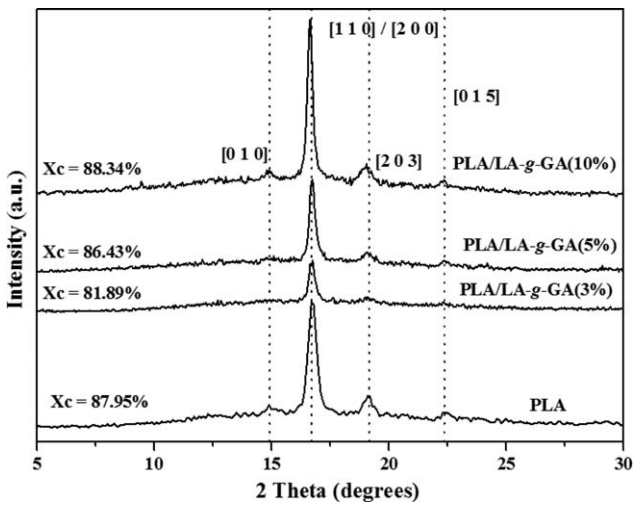

Figure 3. XRD patterns for PLA, PLA/LA-*g*-GA (3%), PLA/LA-*g*-GA (5%), and PLA/LA-*g*-GA (10%) bionanocomposite films.

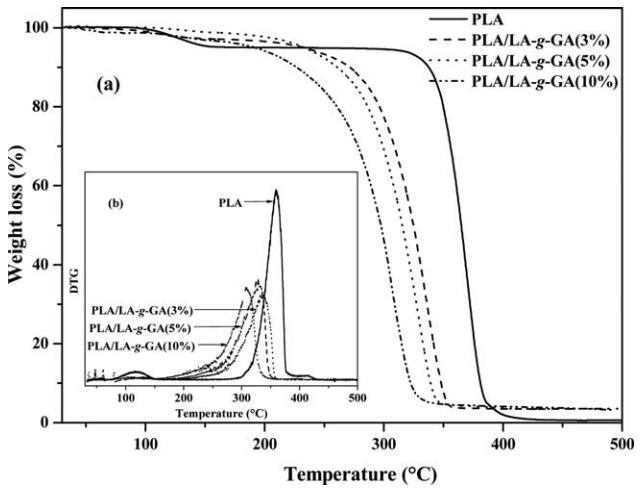

Figure 4. (a) TGA thermograms and (b) DTG curves of PLA and PLA/LA-*g*-GA bionanocomposite films.

samples. The peak obtained in the XRD pattern of PLA/LA-*g*-GA (10%) showed higher intensity, with respect to PLA film, suggested that oligomer promoted crystallization without changing the crystal structure.

Thermal Analysis

TGA was conducted for PLA, PLA/LA-*g*-GA (3%), PLA/LA-*g*-GA (5%), and PLA/LA-*g*-GA (10%) films under inert atmosphere. In the derivative thermogravimetric (DTG) curves, two peaks were observed at different temperatures for neat PLA films, which denote the different weight losses during heating at different temperatures. In neat PLA film, the first broad peak in the temperature range of 75–155 °C indicated the removal of unbound moisture. No such peak was observed up to 150 °C in any PLA/LA-*g*-GA films, which confirmed that bound and unbound moisture were negligible therein. However, the second prominent peak as observed in neat PLA film at 230–440 °C was found in all the samples of PLA/LA-*g*-GA films also with varying heights indicative of their thermal stability. Highest thermal stability was observed for neat PLA films, and on increase in the loading of the filler, decrease in the thermal stability was observed. This could be attributed to the presence of low molecular weight species of oligomer in PLA/LA-*g*-GA films. The onset and offset temperatures for neat PLA films were observed at 315 °C and 375 °C. The onset-offset temperature ranges for PLA/LA-*g*-GA (3%), PLA/LA-*g*-GA (5%), and PLA/LA-*g*-GA (10%) were 171–356 °C, 177–346 °C, and 157–338 °C, respectively. The weight loss percentage in these temperature ranges was approximately 73%, 93%, 93%, and 92% for PLA, PLA/LA-*g*-GA (3%), PLA/LA-*g*-GA (5%), and PLA/LA-*g*-GA (10%) films, respectively, as shown in Figure 4(a). The maximum peak temperature was 359 °C, 336 °C, 328 °C, and 307 °C for PLA, PLA/LA-*g*-GA (3%), PLA/LA-*g*-GA (5%), and PLA/LA-*g*-GA (10%), respectively, as shown in Figure 4(b) which indicated the reduction in thermal stability with increase in the loading of LA-*g*-GA. The weight loss (%) at the corresponding temperatures was approximately 37%, 70%, 72%, and 68% for PLA, PLA/LA-*g*-GA (3%), PLA/LA-*g*-GA (5%), and PLA/LA-*g*-GA (10%), respectively. The huge weight loss in blend films was observed as compared to that of neat PLA films, which confirmed the reduction in thermal stability due to incorporation of short chain LA-*g*-GA in the PLA matrix. The residual weight percent for PLA, PLA/LA-*g*-GA (3%), PLA/LA-*g*-GA (5%), and PLA/LA-*g*-GA (10%) was observed as 0.6%, 3.54%, 3.52%, and 3.19%, respectively. For the PLA/LA-*g*-GA films, around 3% residual weight was observed because of the presence of salts and minerals in GA.[24] It was also observed that the degradation temperatures in all the PLA/LA-*g*-GA films were around 300 °C, which was higher than the processing temperature of neat PLA film. Thus, PLA/LA-*g*-GA films could be processed at the same temperature as neat PLA films.

Through DSC studies, structural arrangement and torsion oscillation of molecular backbone of polymers can be explained by T_g. Figure 5 presents the thermogram for second heating cycles.

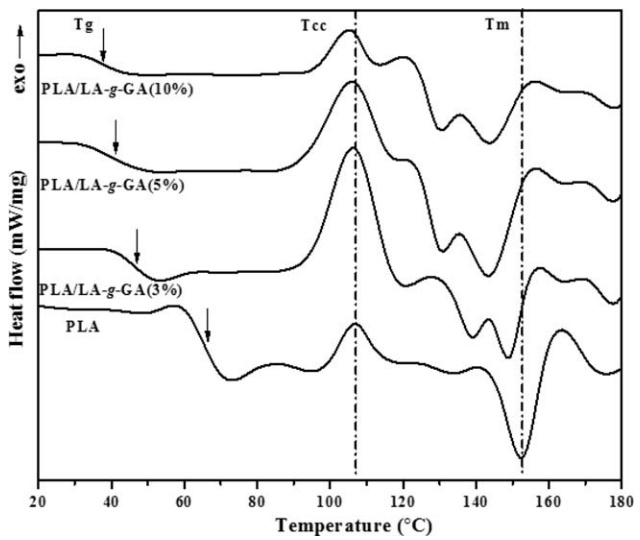

Figure 5. DSC themograms of PLA and PLA/LA-*g*-GA bionanocomposite films during second heating at 5 °C/min.

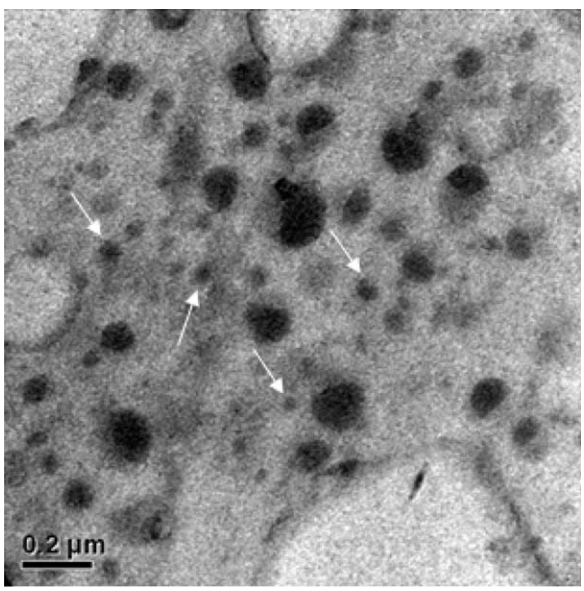

Figure 6. Representative TEM micrograph of PLA/LA-*g*-GA (5%) bionanocomposite film.

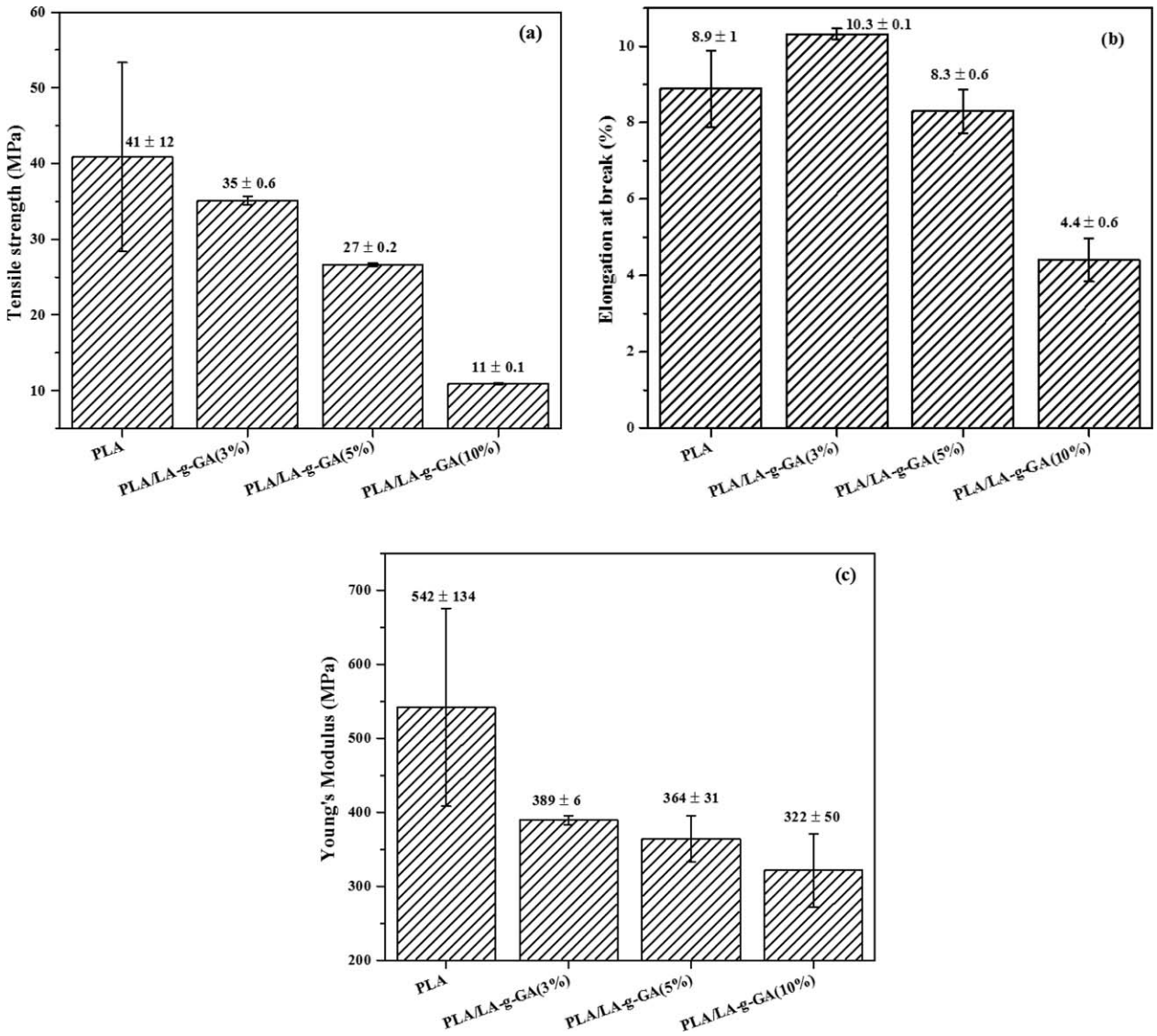

Figure 7. Mechanical properties of film samples (a) tensile strength, (b) elongation at break, and (c) Young's modulus (the error bars represent standard deviations).

The observed T_g for PLA, PLA/LA-*g*-GA (3%), PLA/LA-*g*-GA (5%), and PLA/LA-*g*-GA (10%) were found to be 64.8 °C, 46.4 °C, 41.8 °C, and 41.0 °C, respectively. The DSC thermogram shows that the reduction in T_g took place as the filler concentration was increased. With increase in concentration of the oligomer, magnitude of plasticizing effect increased which was due to enhancement in molecular segmental mobility resulting in reduction in T_g values.

In addition, reduction in regularity and crystalline growth was found hindered. This was because of small and irregular branching of LA-*g*-GA molecules. Single T_g was observed in all the film samples that suggested a good compatibility of LA-*g*-GA (filler) with PLA. As the filler was incorporated in the PLA matrix, an increase in free volume resulted in reduction in T_g values of blend films with respect to neat PLA film. The cold crystallization temperature (T_{cc}) for neat PLA film was observed to be at 107 °C and the same for PLA/LA-*g*-GA films was found to be at 106.99 °C. With increase in the concentration of oligomer molecular chains, broadness of cold crystallization peak increased. The endothermic peak for PLA, PLA/LA-*g*-GA (3%), PLA/LA-*g*-GA (5%), and PLA/LA-*g*-GA (10%) were observed at 153 °C, 149 °C, 143 °C, and 143 °C, respectively. In the PLA/LA-*g*-GA films, two distinct peaks were observed, which indicated the presence of less ordered crystal structures. Thus, at lower temperatures, peaks were formed because of thinner crystalline lamella and at higher temperatures, sharper peaks confirmed about the melting of more perfect crystals. Figure 5 also suggests that as the oligomer concentration increased, the peaks became broader and shifted towards lower temperature, which confirmed the increase in irregularity in crystals.

Surface Morphology

Transmission electron microscopy (TEM) was conducted to analyze the dispersion of nanoparticles in the matrix as shown in Figure 6. Nicely and homogenously dispersed nanometer

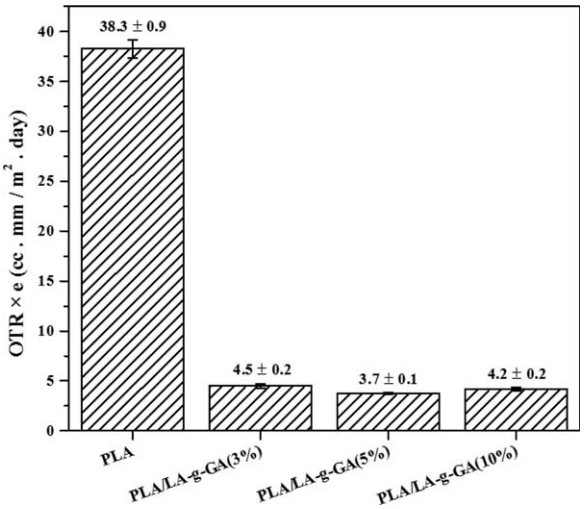

Figure 8. Oxygen transmission rate (OTR × e) value of neat PLA and PLA/LA-*g*-GA bionanocomposite films.

range particles were observed in the PLA matrix, which resulted in drastic enhancement of the oxygen barrier property.

Mechanical Properties

The mechanical properties of PLA and PLA/LA-*g*-GA films were evaluated for tensile strength, elongation at break, and Young's modulus, and their values have been presented as in Figure 7. The obtained values of tensile strength, elongation at break, and Young's modulus were 40.9 MPa, ~9%, and 541.91 MPa, respectively, for neat PLA films. It was observed that with increase in the filler concentration, reduction in tensile strength of the films occurred [Figure 7(a)]. In PLA/LA-*g*-GA (3%) films, 14% reduction in tensile strength with respect to neat PLA films was observed. This could be due to the presence of short oligomer chains in PLA matrix and LA-*g*-GA filler, which are contributing towards poor interaction due to reduction in chain entanglement effect with PLA interphase, as shown in Figure 7(a).[25,26]

The enhancement of 16% in elongation at break (ε_b) was observed for PLA/LA-*g*-GA films with respect to neat PLA films. Addition of 3 wt % filler loading reduced intermolecular forces, which increased the flexibility of PLA/LA-*g*-GA (3%) films, due to the plasticizing effect of oligomers as shown in Figure 7(b). On further addition of oligomer concentration, 7% and 50.5% reduction in elongation at break were observed for PLA/LA-*g*-GA (5%) and PLA/LA-*g*-GA (10%) films respectively. Thus, as small molecules of the oligomer interact with long chain of polymer molecules, 'free volume' was generated between the long polymer chains. Such interaction results in weakening intermolecular forces between the polymer chains or decreased in entanglement in molecular chains of the neat PLA matrix. These small molecules of oligomer were responsible for increase in the distance between two polymer chains. This could also be ascribed to phase separation between the oligomer and PLA matrix.

Young's modulus was reduced by 28.2, 32.8, and 40.7% on addition of 3, 5, and 10% LA-*g*-GA filler, respectively, as shown in Figure 7(c). Furthermore, with increase in the filler concentration, reduction in polymer homogeneity leads to reduction in tensile strength and Young's modulus in PLA/LA-*g*-GA films. Thus, increase in oligomer concentration reduced the stiffness of the films.

Oxygen Permeability

Figure 8 presents the oxygen transmission rate (OTR); OTR × e values obtained for PLA and PLA/LA-*g*-GA films. A very significant decrease in OTR values was observed when oligomer was added to the polymer matrix. The PLA/LA-*g*-GA films showed an enhanced barrier effect due to their good dispersion as shown in Figure 6. PLA/LA-*g*-GA films with 3%, 5%, and 10% loading showed 88.3, 90.3, and 89.1% reduction in OTR × e values, respectively, with respect to the PLA films. This was in accordance with the results obtained in surface morphology, where it was observed that the presence of microspheres causes discontinuity in the film matrix and increases the tortuosity in the probable oxygen path to prevent permeation of gas molecules. It is noteworthy to mention here that due to uniform dispersion of LA-*g*-GA in the PLA matrix, it reduces the solubility of oxygen molecules in the bionanocomposites and hence, the combine effect of tortuosity and solubility leads to the significant reduction in oxygen permeability. However, it was possible to observe that, in PLA/LA-*g*-GA (10%) film, the oxygen permeation increased slightly which could be attributed to agglomeration of microspheres that lead to reduction in tortuosity.

Water Vapor Transmission Rate

WVTR × e of PLA and PLA/LA-*g*-GA films are shown in Figure 9. The decrease in WVTR × e was observed when the filler was blended with the PLA matrix. The reduction in WVTR × e for PLA/LA-*g*-GA (3%) films was observed around 7% and on further addition of the filler that is for PLA/LA-*g*-GA (5%) was around 27%. This drastic decrease in the values was due to the presence of micro and nanospheres present in the matrix. Hence, the tortuous path created by these spheres helped in the sudden decrease in the WVTR × e also. On the contrary, drastic increase in WVTR × e was observed around 28% for PLA/

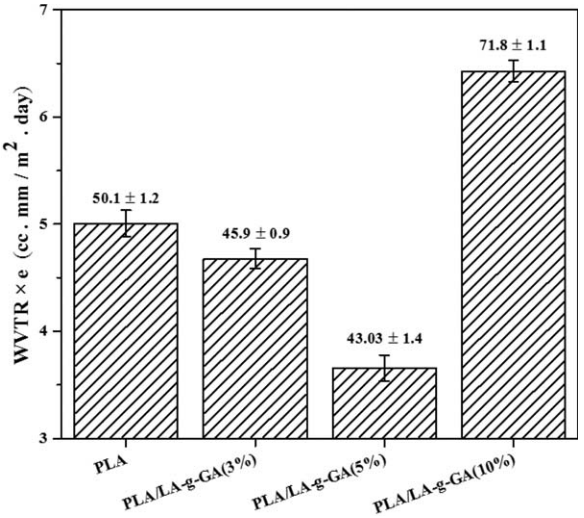

Figure 9. Water vapor transmission rate (WVTR × e) of neat PLA and PLA/LA-*g*-GA bionanocomposite films.

LA-*g*-GA (10%) films with respect to neat PLA films. This was observed due to agglomeration of micro and nanospheres, which resulted in reduction in tortuosity. The decrease in intermolecular forces was also occurred in PLA/LA-*g*-GA (10%) films due to free hydroxyl and carboxyl groups of the filler. Thus, increase in transfer of water molecules through the films was observed.

CONCLUSIONS

A novel polysaccharide gum based filler was synthesized by using lactic acid and gum arabic as precursors. The synthesis was conducted by polycondensation reaction without using any catalyst or additive. The grafting occurred at -OH and -NH_2 groups which was confirmed by NMR analysis. The PLA and PLA/LA-*g*-GA bionanocomposite films were prepared by solution casting method. PLA was found to be compatible with the LA-*g*-GA filler that was confirmed by single T_g of the polymeric blends obtained by mixing the two materials in different proportions. Reduction in the glass transition temperature is indicating that these films are good for packaging applications. However, magnitude of reduction in the values of these properties was dependent on the percentage of LA-*g*-GA. However, for 3% filler loading the film observed the highest elongation at break as ~10% which is even greater than that of neat PLA film. The presence of nanospheres is confirmed by TEM images, which clearly inferred that blending of LA-*g*-GA to PLA significantly altered the morphological characteristics of the film. The reduction in WVTR analysis for PLA/LA-*g*-GA (3%) and PLA/LA-*g*-GA (5%) films was observed as 7% and 27%, respectively. The most important achievement of this work is the significant improvement in the oxygen transmission rate (OTR) of composite films. The OTR × e value of neat PLA films was 37.6 cm^3 mm m^{-2} day^{-1}, which is reduced to around 4 cm^3 mm m^{-2} day^{-1}. A decrease of ~10 fold in the OTR value can be regarded as very significant improvement in the barrier property of the film, especially for using them as packaging films. In addition to extremely low OTR × e values of prepared films, GA and PLA that are obtained from natural renewable resources, are possibly non-toxic, and fit well in the category of 'green' biodegradable materials for high quality packaging materials.

ACKNOWLEDGMENTS

Authors gratefully acknowledge the Centre of Excellence for Sustainable Polymers (CoE-SusPol) funded by Department of Chemicals and Petrochemicals (DCPC), Central Instruments Facility (CIF), and Department of Chemical Engineering at Indian Institute of Technology Guwahati (IITG), India for providing research and analytical facilities.

REFERENCES

1. Sevigne-Itoiz, E.; Gasol, C. M.; Rieradevall, J.; Gabarrell, X. *Waste Manage.* **2015**, *46*, 557.
2. Gonzalez, A.; Igarzabal, C. I. A. *Food Hydrocolloids* **2013**, *33*, 289.
3. Rhim, J. W.; Park, H. M.; Ha, C. S. *Progr. Polym. Sci.* **2013**, *38*, 1629.
4. Cutter, C. N. *Meat Sci.* **2006**, *74*, 131.
5. Ramos, M.; Jimenez, A.; Peltzer, M.; Garrigos, M. C. *Food Chem.* **2014**, *162*, 149.
6. Auras, R.; Harte, B.; Selke, S. *Macromol. Biosci.* **2004**, *4*, 835.
7. Goncalves, C. M. B.; Tome, L. C.; Garcia, H.; Brandao, L.; Mendes, A. M.; Marrucho, I. M. *J. Food Eng.* **2013**, *116*, 562.
8. Rudnik, E.; Briassoulis, D. *Ind. Crops Prod.* **2011**, *33*, 648.
9. Burgos, N.; Martino, V. P.; Jimenez, A. *Polym. Degrad. Stab.* **2013**, *98*, 651.
10. Arrieta, M. P.; Fortunati, E.; Dominicib, F.; Lopez, J.; Kenny, J. M. *Carbohydr. Polym.* **2015**, *121*, 265.
11. Bonilla, J.; Fortunati, E.; Vargas, M.; Chiralt, A.; Kenny, J. M. *J. Food Eng.* **2013**, *119*, 236.
12. Raquez, J. M.; Habibi, Y.; Murariu, M.; Dubois, P. *Progr. Polym. Sci.* **2013**, *38*, 1504.
13. Reddy, M. M.; Vivekanandhan, S.; Misra, M.; Bhatia, S. K.; Mohanty, A. K. *Progr. Polym. Sci.* **2013**, *38*, 1653.
14. Ali, A.; Maqbool, M.; Ramachandran, S.; Alderson, P. G. *Postharvest Biol. Technol.* **2010**, *58*, 42.
15. Wang, H.; Williams, P. A.; Senan, C. *Food Hydrocolloids* **2014**, *37*, 143.
16. Nie, S. P.; Wang, C.; Cui, S. W.; Wang, Q.; Xie, M. Y.; Phillips, G. O. *Food Hydrocolloids* **2013**, *31*, 42.
17. Tsai, R. Y.; Chen, P. W.; Kuo, T. Y.; Lin, C. M.; Wang, D. M.; Hsien, T. Y.; Hsieh, H. *J. Carbohydr. Polym.* **2014**, *101*, 752.
18. Duncan, T. V. *J. Colloid Interface Sci.* **2011**, *363*, 1.
19. Segal, L.; Creely, J. J.; Martin, A. E., Jr.; Conrad, C. M. *Text. Res. J.* **1959**, *29*, 786.
20. Zhao, Y.; Qiu, J.; Feng, H.; Zhang, M.; Lei, L.; Wu, X. *Chemical Eng. J.* **2011**, *173*, 659.
21. Park, S.; Baker, J. O.; Himmel, M. E.; Parilla, P. A.; Johnson, D. K. *Biotechnol. Biofuels* **2010**, *3*, 1.
22. Wang, Z.; Zheng, L.; Li, C.; Zhang, D.; Xiao, Y.; Guana, G.; Zhu, W. *Carbohydr. Polym.* **2013**, *94*, 505.
23. Haafiz, M. K. M.; Hassan, A.; Zakaria, Z.; Inuwa, I. M.; Islam, M. S.; Jawaid, M. *Carbohydr. Polym.* **2013**, *98*, 139.
24. Ali, B. H.; Ziada, A.; Blunden, G. *Food Chem. Toxicol.* **2009**, *47*, 1.
25. Chou, P. M.; Mariatti, M.; Zulkifli, A.; Sreekantan, S. *Compos. B* **2012**, *43*, 1374.
26. Silverajah, V. S. G.; Ibrahim, N. A.; Zainuddin, N.; Yunus, W. M. Z. W.; Hassan, H. A. *Molecules* **2012**, *17*, 11729.